Journal of Applied Polymer Science

Isothermal emulsion polymerization of *n*-butyl methacrylate with KPS and redox initiators: Kinetic study at different surfactant/initiator concentrations and reaction temperature

Shi Wang,[1,2] Eric S. Daniels,[1] E. David Sudol,[1] Andrew Klein,[1,2] Mohamed S. El-Aasser[1,2]
[1]Emulsion Polymer Institute, Lehigh University, Bethlehem, Pennsylvania 18015
[2]Department of Chemical Engineering, Lehigh University, Bethlehem, Pennsylvania 18015
Correspondence to: M. S. El-Aasser (E-mail: mse0@lehigh.edu)

ABSTRACT: Thermal initiators, although widely used in emulsion polymerization, are limited to high reaction temperatures due to their high activation energy. Redox initiators have low activation energies indicating that emulsion polymerization could be conducted at lower temperatures to save energy. In the present study, a redox initiator system comprised of hydrogen peroxide (H_2O_2) and ascorbic acid (AA) in conjunction with a Fe^{2+} ion catalyst is compared with a potassium persulfate (KPS) thermal initiator in an emulsion polymerization system consisting of *n*-butyl methacrylate (BMA), sodium lauryl sulfate (SLS) and water. The dependence of particle number on surfactant and initiator concentrations shows that redox- and KPS-initiated systems both follow the Smith-Ewart theory. However, the high radical flux generated from the redox initiator results in the formation of much smaller latex particles and higher reaction rate with lower molecular weights. Latex particle size and molecular weight could also be influenced by reaction temperature. By using redox initiator, small monodisperse particles (diameter < 50 nm) can be achieved without using a large amount of surfactant. © 2015 Wiley Periodicals, Inc. J. Appl. Polym. Sci. **2016**, *133*, 43037.

KEYWORDS: colloids; emulsion polymerization; kinetics; radical polymerization

Received 2 July 2015; accepted 12 October 2015
DOI: 10.1002/app.43037

INTRODUCTION

Emulsion polymerization is an important method to produce latex polymers in industry. Many commodity polymers are prepared by the emulsion polymerization process, such as synthetic rubber, latex paints, paper coatings, adhesives and binders for non-woven fabrics.[1,2] World demand for emulsion polymers is forecast to rise 5.2 percent per year to 12.8 million metric tons in 2014.[3] In recent years, the field of polymer colloids has expanded rapidly in many applications, such as biotechnology, medicine, sensors, printing, catalysts, etc.[4–10] For these novel applications, employing small monodisperse particles can result in better performance. Therefore, high surfactant concentration, low solids and some radiation methods (microwave) have been used to synthesize latex particles that are smaller than 50 nm.[11–13] However, those methods have limitations in larger scale latex production.

In conventional thermally initiated isothermal emulsion polymerizations, high temperatures (60–90°C) are usually employed to maintain process stability and reproducibility and to reduce the polymerization cycle time. The energy used in the commercial-scale processes is large, and the cost is high to carry out the high-temperature isothermal reaction.[14,15] By using a redox initiator, radicals can be generated at room temperature due to their low activation energies[16] of ~40–80 kJ·mol^{-1}. Therefore, redox-initiated reactions associated with adiabatic conditions can be started at a lower temperature leading to reduction of energy costs, equipment costs, and reaction cycle time. To study the kinetics of the current emulsion polymer system, isothermal conditions were used to reduce the complexity of the analysis.

In conventional thermally-initiated emulsion polymerization, the particle size can range from 50 to 500 nm. A redox initiator system can be an alternative process to effectively synthesize monodisperse latex particles with a size smaller than 50 nm in emulsion polymerization. Compared with thermal initiators, redox initiators generate a high radical flux during the reduction-oxidation reaction and could result in the formation of smaller particles at low surfactant concentrations and high solids content.[17,18] There are many advantages of using redox initiators in emulsion polymerization process. However, kinetic studies of redox initiator in emulsion polymer systems are very limited.

To study redox-initiated emulsion polymerization, a redox initiator system comprised of hydrogen peroxide (H_2O_2) and ascorbic acid (AA) in conjunction with Fe^{2+} ion catalyst is compared with a potassium persulfate (KPS) thermal initiator in the emulsion polymerization of n-butyl methacrylate (BMA). *n*-Butyl methacrylate (BMA) monomer is a well-studied monomer[19–24] with high propagation rate constant[25] and low water solubility.[26] The H_2O_2/AA/Fe^{2+} redox system[27–30] is widely used in industry as well as in research. The Mettler RC1 reactor calorimeter was used to carry out the emulsion polymerization. During the polymerization, the reaction heat was measured and the reaction rate was calculated. In previous work,[21,22] emulsion polymerization of BMA using SLS surfactant and KPS initiator were studied by the Mettler RC1 reactor calorimeter with limited data. To better study the nucleation and kinetics of emulsion polymerization of BMA, a series of reactions with different surfactant concentrations, initiator concentrations and reaction temperatures were carried out to compare the influence of the KPS and redox initiators on the polymerization kinetics, particle size and molecular weight.

In this study, monodisperse, small (less than 50 nm) latex particles were produced by using redox initiator. The dependence of particle number on surfactant and initiator concentrations shows that redox and KPS-initiated systems both follow the Smith-Ewart theory,[31] which indicates that micellar nucleation occurs in both systems. The high radical flux generated from the redox initiator decomposition results in the formation of smaller latex particles with lower molecular weights.

EXPERIMENTAL

Materials

The monomer, *n*-butyl methacrylate (*n*-BMA) (Acros), was purified via vacuum distillation in the presence of cuprous chloride at 40 mmHg and 70°C to remove any inhibitor and oligomers present in the monomer before use. All other materials were used as received without further purification, including the thermal initiator, potassium persulfate (KPS, Fisher Scientific), the redox initiator system, 30 wt % hydrogen peroxide (H_2O_2, Mallinckrodt Chemicals) and L-ascorbic acid (AA, Sigma-Aldrich), the redox initiator catalyst, ferrous sulfate (Fisher), the surfactant, sodium lauryl sulfate (SLS, MP Biochemicals), the buffer salt, sodium bicarbonate ($NaHCO_3$, Mallinckrodt), the polymer solvent, tetrahydrofuran (THF, J. T. Baker), ionic strength buffer, sodium chloride (Sigma-Aldrich), and inhibitor, hydroquinone (HQ, Sigma-Aldrich) to terminate polymerization in the samples removed from the reactor for determination of conversion vs. time. Deionized water (DIW, Barnstead NANO pure II system) with a conductivity below 0.8 μs was used in all experiments.

KPS-Initiated Emulsion Polymerization

The Metter RC1 reactor calorimeter equipped with a pitched-blade impeller and one baffle was used to carry out the KPS-initiated isothermal polymerizations at an agitation speed of 400 rpm. The reaction temperature was predominantly maintained at 70°C, and other reaction temperatures of 55°C or 85°C were also utilized to study the effect of temperature on the polymerization. 125 g *n*-BMA monomer and 500 g DIW were charged into the reactor followed by various amounts of SLS surfactant and $NaHCO_3$ buffer salt. Nitrogen gas was then bubbled into the solution for 5 min in order to remove oxygen. After shutting off the nitrogen inlet and outlet, the reactor temperature was increased to the desired temperature, and then 5 mL of KPS aqueous initiator solution was fed into the reactor in one shot. In order to study the initiator strength dependence, the KPS concentration was varied in a range from 0.43 m*M* to 6.8 m*M* in the initiator solution. The mass ratio of KPS and $NaHCO_3$ buffer salt was maintained at 1:1. The recipes for KPS-initiated emulsion polymerization are shown in Table I.

Table I. Recipes Used for the KPS-Initiated Emulsion Polymerization of BMA

Ingredient	Amount
BMA	125 g
DI water	500 g
SLS	0.578–5.776 g (4.0–40.0 m*M*)[a]
KPS	0.058–0.937 g (0.43–6.8 m*M*)[a]
$NaHCO_3$	0.058–0.937 g (1.4–22.4 m*M*)[a]
Reaction Temperature	55–85°C

[a] Based on the aqueous phase.

Redox-Initiated Emulsion Polymerization

The redox-initiated isothermal emulsion polymerizations were also carried out in the Mettler RC1 reactor calorimeter with the same configuration as described previously. The reaction temperature was predominantly maintained at 25°C, and other temperatures of 40°C or 55°C were applied to study the effect of reaction temperature in the redox-initiated system. All procedures were the same as in the KPS-initiated emulsion polymerizations before adding redox initiators except that a ferrous sulfate solution was also charged into the reactor and the buffer salt was replaced with 7.2 m*M* NaCl before nitrogen gas bubbling. The redox initiator in this study contains AA and H_2O_2. The two substances were dissolved in 5 g water, respectively, and fed separately into the reactor in one shot. The H_2O_2 solution was fed into the reactor first and the ascorbic acid solution was fed one minute later. The mass ratio of AA and 30 wt % H_2O_2 was maintained at a 1:1 ratio to study the influence of

Table II. Recipes Used for the Redox-initiated Emulsion Polymerization of BMA

Ingredient	Amount
BMA	125 g
DI water	500 g
SLS	0.578–5.776 g (4.0–40.0 m*M*)[a]
$FeSO_4$	0.0125 g (0.09 m*M*)[a]
NaCl	0.209 g (7.2 m*M*)[a]
AA	0.05–0.90 g (0.6–10.2 m*M*)[a]
H_2O_2 (30%)	0.06–0.90 g (1.0–15.8 m*M*)[a]
Reaction Temperature	25–55°C

[a] Based on the aqueous phase

redox initiator concentration. The recipes for redox-initiated emulsion polymerization are shown in Table II.

After the polymerization was complete, one drop of 1.0% aqueous hydroquinone solution was used to terminate further reaction in the sample pan. Samples of 10 gram each were then taken for measurements of particle size, conversion and molecular weight.

Characterization

The final polymerization conversion (x) was determined by gravimetric analysis of the final latex.[32] A given amount of latex was weighed out into an aluminum sample pan and dried at 70°C overnight, and the remaining solids was weighed. The solids content (X) and the conversion (x) were calculated using eqs. (1) and (2):

$$X = \frac{m_2 - m_0}{m_1 - m_0} \tag{1}$$

$$x = \frac{X \times (m_w + m_{\text{initiator}} + m_{\text{BMA}} + m_{\text{buffer}}) - (m_{\text{initiator}} + m_{\text{buffer}})}{m_{\text{BMA}}} \tag{2}$$

where m_0 is the mass of the empty aluminum pan, m_1 is the mass of the aluminum pan with the latex, m_2 is the mass of the aluminum pan after drying, and m_w, $m_{\text{initiator}}$, m_{BMA}, and m_{buffer} are the masses of water, initiator, BMA monomer, and buffer salt added prior to the reaction, respectively.

The molecular weight and molecular weight distribution were measured by gel permeation chromatography (GPC) using a Waters 515 HPLC Pump, Waters 410 differential refractometer detector (2487 Dual λ Absorbance Detector) and Waters Styragel columns (HR3, HR4 and HR6). The latex was dried in the oven (70°C) for 48 h, and then dissolved in THF (1.5 wt %). The polymer solution was filtered with a 0.45 μm PTFE filter before injection into the GPC. THF was used as the eluent at a flow rate of 1 mL/min, and polystyrene standards were used for calibration. The number-average molecular weight (M_n), weight-average molecular weight (M_w), and polydispersity index (PDI = M_w/M_n) were obtained.

Transmission electron microscopy (TEM, JEOL 2000) was used to obtain images of the latex particles. One drop of the latex sample was diluted in 15 g DI water using a plastic pipette. Then 15 drops of 2.0 wt % phosphotungstic acid negative stain were added in order to prevent the particles from deforming during TEM imaging at high voltage. A drop of the diluted and stained latex was added onto a copper grid (Ernest F. Fullam, Inc.) and dried at room temperature before the TEM imaging. An electron beam with an accelerating voltage of 200 kV was used with a magnification range from 50 k to 200 k.

For each latex sample, about 1000 particles in the TEM images were measured to obtain statistical results of particle size and size distribution. The measurement of particle size for each sample used more than 5 different TEM images under the same TEM operating parameters. The number-average diameter (D_n), volume-average diameter (D_v), weight average-diameter (D_w), standard deviation, and particle size polydispersity index (PDI) were statistically calculated based on the measured particle sizes.[33] The volume-average diameter, D_v (m), was used to calculate the final particle number, N_f (L^{-1}), i.e.,

$$N_f = \frac{6 m_{BMA} x}{\rho \pi D_v^3 V} \tag{3}$$

where m_{BMA} (kg) is the mass of the initial BMA, ρ (kg/m^3) is the density of the polymer (PBMA: 1.053 x 10^3), and V (L) is the volume of the latex.

The heat of reaction, Q_r, was recorded by the Mettler RC1 reaction calorimeter, and used to calculate the rate of reaction (R_p) [eq. (4)] and the fractional conversion (x_t) [eq. (5)] at any time during the polymerization,[34]

$$R_{\text{p}} = \frac{Q_{\text{r}}}{\Delta H_{\text{p}} V_{\text{w}}} \tag{4}$$

$$x_t = \frac{M_0 \int_0^t Q_{\text{r}} \text{d}t}{\Delta H_{\text{p}} m_{BMA}} \tag{5}$$

where $\triangle H_p$ is the heat of polymerization (J/mol), V_w is the volume of water in the RC1 reactor (dm^3), M_0 (g/mol) is the molecular weight of the monomer, and m_{BMA} (g) is the mass of the BMA monomer prior to the reaction.

RESULTS AND DISCUSSION

In the redox-initiated emulsion polymerizations of BMA, it is very important to have ferrous ion present in the redox system since it reacts with hydrogen peroxide and facilitates radical generation.[27] The reaction rate is much lower and an induction period occurs in the redox-initiated emulsion polymerization without ferrous ions present.[35] Therefore, ferrous ion (concentration of 0.09 mM) was used in the recipes to ensure a consistent radical generation rate.

Reaction Kinetics

The reaction kinetics of KPS-initiated and redox-initiated polymerizations are shown in Figure 1 (a,b). The plot shows the influence of the SLS surfactant concentration. Three intervals[1] (I, II, and III) are clearly shown in the KPS-initiated polymerization [Figure 1(a)]. At the beginning of the reaction, the process of micellar nucleation results in a very fast increase in the reaction rate (Interval I). Once the conversion is over 5%, the nucleation process is almost complete and the reaction rate becomes more or less constant (Interval II). After 40% conversion, the reaction rate decreases due to the disappearance of the monomer droplets (Interval III). At low surfactant concentrations of 4, 6, and 7.8 mM, the later stage of Interval III shows an increase in reaction rate caused by the gel effect or Trommsdorff-Norrish effect[1] (around 90% conversion). A similar reaction rate profile was reported by Krishnan *et al.*[22] The concentration of polymer at high conversion increases resulting in a high viscosity inside the latex particles, and thus leads to the decrease of termination rate and increase of the propagation rate, i.e., the gel effect. The gel effect has a smaller influence on reaction rate for latex with smaller particle size. Surfactant at high concentrations forms a larger number of micelles and leads to a larger number of small particles. Therefore, faster reaction

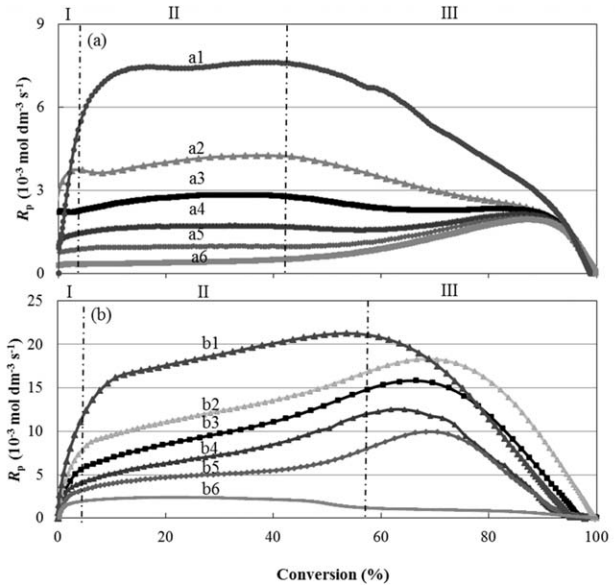

Figure 1. The dependence of reaction rate on surfactant (SLS) concentrations in the KPS and redox-initiated emulsion polymerization of BMA. Figure 1(a) represents 1.7 m*M* KPS-initiated reactions at 70°C, and Figure 1(b) represents redox-initiated reactions with 5.1 m*M* AA and 7.9 m*M* H_2O_2 at 25°C. SLS concentration levels: a1 & b1: 40 m*M*, a2 & b2: 20 m*M*, a3 b3: 12 m*M*, a4 & b4: 7.8 m*M*, a5 & b5: 6 m*M*, and a6 & b6: 4 m*M*. All reactions have a solids content of 20 wt % BMA. I, II, and III represent three Intervals during emulsion polymerization.

rates with no gel effect were observed at high surfactant concentrations (curves a1 & a2).

However, the three intervals in the redox-initiated polymerizations are not present at the same conversion as in the KPS-initiated reactions. Figure 1(b) shows a fast increase in reaction rate at the beginning of the reaction (Interval I). However, the reaction rate increases continuously with a slower rate during Interval II until reaching ~70% conversion. The increase of reaction rate in Interval II indicates a significant continuation of nucleation following the initial nucleation in Interval I, and this demonstrates that significant secondary nucleation exists in the redox-initiated emulsion polymerization. A fast decrease in the reaction rate was observed in Interval III due to the disappearance of the monomer. Similar to the KPS-initiated reactions, the reaction rate increases with surfactant concentration in the redox-initiated systems. The difference is that the reaction rate in the redox-initiated polymerization is almost 4 times higher compared to the KPS-initiated polymerization. The higher reaction rate can be explained by much greater numbers of particles generated in the redox-initiated polymerization.

Figure 2(a,b) show the influence of initiator concentration on the reaction kinetics of KPS-initiated and redox-initiated emulsion polymerizations, respectively. The three intervals defined by initiation of emulsion polymerization (sharp reaction rate increase), propagation (slower reaction rate increase) and disappearance of monomer (decrease of reaction rate) were clearly shown for all KPS-initiated and redox-initiated polymerizations, which were described before. However, the redox-initiated polymerizations have different interval shapes and magnitudes of reaction rate. Figure 2(a,b) also indicate that the reaction rate is higher with higher initiator concentrations. Higher initiator concentration results in a higher radical generation rate, and thus, higher particle numbers. The high particle number leads to a high reaction rate. The higher initiator concentration also resulted in a large increase in the reaction rate during Interval II, which indicates that secondary nucleation is influenced by the radical generation rate.

The influence of reaction temperature on the reaction kinetics of KPS-initiated and redox-initiated polymerizations are shown in Figure 3(a,b), respectively. The three reaction intervals were again clearly illustrated for the KPS-initiated and redox-initiated polymerization, where the redox-initiated polymerizations have different interval shapes and magnitude of reaction rate. For both KPS-initiated and redox-initiated polymerizations, the reaction rates increase with reaction temperature. High temperature leads to a high reaction rate constant and high radical generation rate with higher particle number, and thus results in fast reaction rate. The higher radical generation rate at higher reaction temperature also resulted in a large increase in the rate of reaction during Interval II. This confirms that secondary nucleation is influenced by the radical generation rate.

Particle Size and Particle Number

Figure 4 represents the TEM images of latex particles obtained from reactions carried out with a SLS concentration of 12.0 m*M* at 70°C and 1.7 m*M* KPS [Figure 4(a)] and at 25°C and 7.9 m*M* H_2O_2 [Figure 4(c)]. Both redox-initiated and KPS-

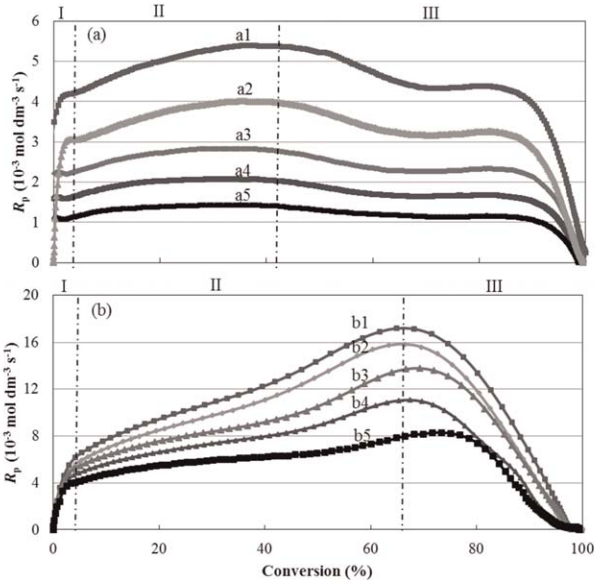

Figure 2. The dependence of reaction rate on initiator concentrations in the KPS and redox-initiated emulsion polymerization of BMA. Figure 2(a) represents KPS-initiated reactions with a SLS concentration of 12.0 m*M* at 70°C, and Figure 2(b) represents redox-initiated reactions with a SLS concentration of 12.0 m*M* at 25°C. KPS concentration levels are: a1: 6.8 m*M*, a2: 3.4 m*M*, a3: 1.7 m*M*, a4: 0.86 m*M*, a5: 0.43 m*M*. H_2O_2 concentration levels: b1: 15.8 m*M*, b2: 7.9 m*M*, b3: 4.0 m*M*, b4: 2.0 m*M*, b5: 1.0 m*M*. All reactions have a solids content of 20 wt % BMA. I, II, and III represent the three Intervals observed during emulsion polymerization.

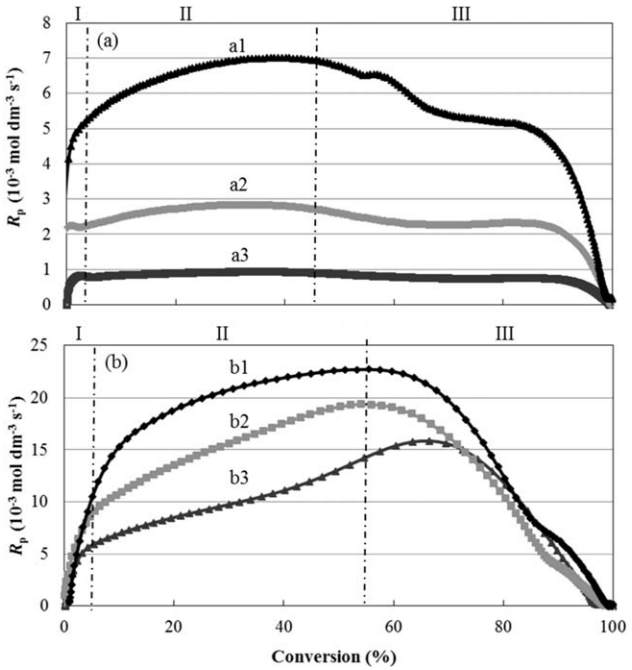

Figure 3. The dependence of reaction rate on reaction temperatures in the KPS and redox-initiated emulsion polymerization of BMA. Figure 3(a) represents 1.7 m*M* KPS-initiated reactions with a SLS concentration of 12.0 m*M*, and Figure 3(b) represents redox-initiated reactions with 12.0 m*M* SLS and 7.9 m*M* H_2O_2. Reaction temperature levels: a1: 85°C, a2: 70°C, a3: 55°C, b1: 55°C, b2: 40°C, and b3: 25°C. All reactions have a solids content of 20 wt % BMA. I, II, and III represent the three Intervals that are observed during emulsion polymerization.

initiated latex particles have a narrow size distributed, whereas the redox-initiated latex has a much smaller particle size. This occurs because redox initiator can generate a much higher radical flux compared to the thermal initiator.

The difference in appearance between the two latexes is significant between the KPS-initiated latex and the redox-initiated latex, as shown in Figure 4. The KPS-initiated latex has a particle diameter of 113 nm [Figure 4(a)] and is white and opaque [Figure 4(b)]. The redox-initiated latex has a particle diameter of 44 nm [Figure 4(c)] and is translucent [Figure 4(d)]. The translucent appearance of the redox-initiated latex indicates less light scattering from the latex due to the smaller particle size, which can also be affected by SLS and initiator concentration. The latex becomes more translucent at higher SLS/initiator concentrations, which produce smaller particle size. By using redox initiator, small latex particles (diameter < 50 nm) with narrow size distributions (PDI < 1.05) can be produced.

Particle number has a reciprocal relation to particle size. The influence of surfactant concentration, initiator strength, and reaction temperature on latex particle number are shown in Figure 5. Figure 5(a) demonstrates that the particle number increases with surfactant concentration for the KPS and redox-initiated reactions. It also shows a turning point of the particle number at the critical micelle concentration (CMC) of SLS surfactant, which is around 7.8 m*M*.[36] This indicates that micellar nucleation is an important nucleation mechanism in the two systems. When the surfactant concentration is above the CMC, the relationship between particle number and surfactant concentration is $N_p \propto C_{SLS}^{0.81}$ for the KPS-initiated latex, and is $N_p \propto C_{SLS}^{0.60}$ for the redox-initiated latex. The Smith-Ewart theory[31] reveals that the relationship (above CMC) between particle number and surfactant concentration is $N_p \propto C_{SLS}^{0.6}$ in micellar nucleation. Since the reactions used different recipes and reaction conditions than those in the Smith-Ewart (S-E) theory, the power dependency value can be different. Therefore, both KPS-initiated and redox-initiated reactions follow the S-E theory.

The influence of initiator concentration was studied next. Since concentration levels are quite different for the KPS and redox initiators, a relative initiator concentration was introduced in order to illustrate their influence on particle number or molecular weight in a single figure [see Figures 5(b), 6(b), and 7(b), respectively]. KPS concentrations were normalized with 1.7 m*M* of the KPS initiator as the base, and H_2O_2 concentrations were normalized with 7.9 m*M* of the redox initiator as the base. These bases were chosen because the initiator concentrations were maintained during the investigation of the other influences that were described previously. Figure 5(b) shows that the particle number increases with initiator concentration. The relationship between particle number and initiator concentration is $N_p \propto C_I^{0.40}$ for the KPS-initiated latex and $N_p \propto C_I^{0.28}$ for the

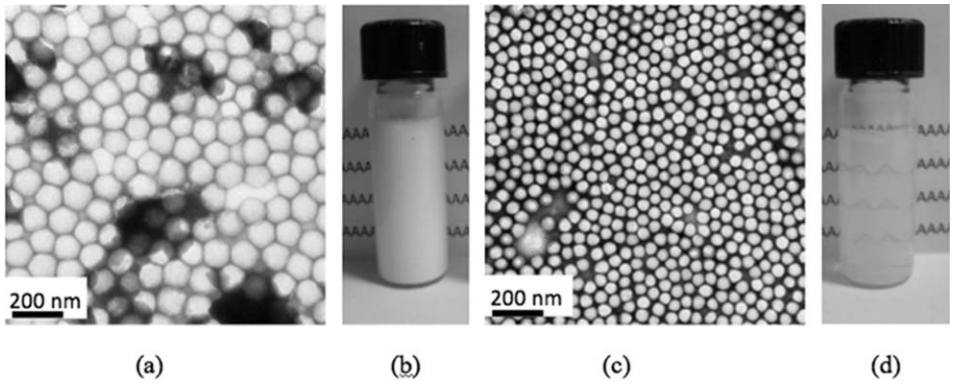

Figure 4. TEM images of (a) KPS-initiated and (c) redox-initiated PBMA latexes and images of (b) KPS-initiated and (d) redox-initiated PBMA latexes. Reaction conditions: 12.0 m*M* SLS, 1.7 m*M* KPS, 7.9 m*M* H_2O_2, 70°C for KPS initiation, 25°C for redox initiation, and 20 wt % BMA.

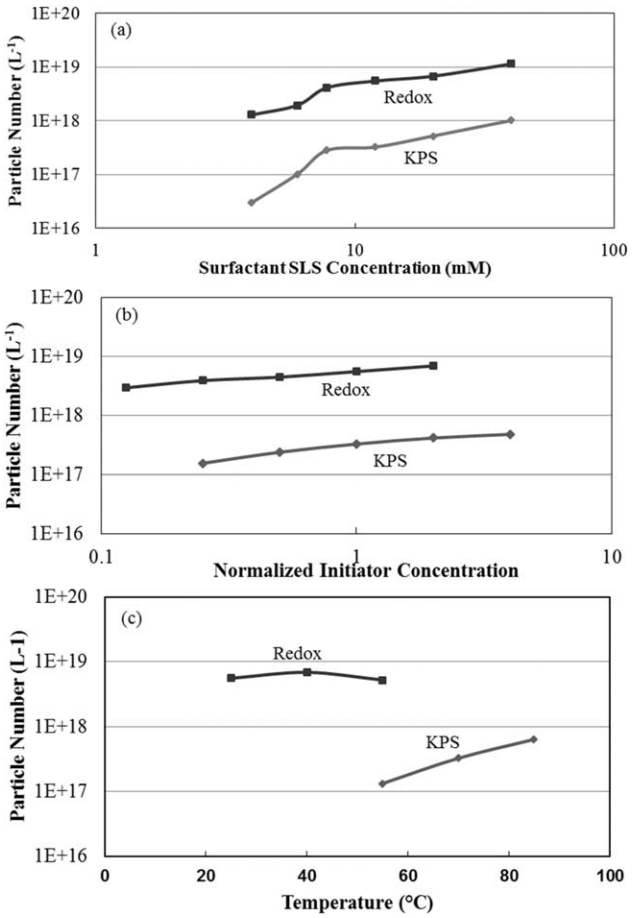

Figure 5. The logarithmic dependence of latex particle number on (a) surfactant SLS concentration, (b) normalized initiator concentration, and (c) reaction temperatures for KPS and redox initiated emulsion polymerizations of *n*-BMA. Reactions represented in (a) were the same as in Figure 1, these in (b) were the same as in Figure 2, and these in (c) were the same as in Figure 3. Initiator concentrations were normalized to those values shown in Figure 5(b).

redox-initiated latex. In the Smith-Ewart theory,[31] the relationship is $N_p \propto C_I^{0.40}$. The relationships between the particle number and initiator/surfactant concentrations indicate that micellar nucleation is operative in both polymerizations.

Reaction temperatures positively affect the particle number of the KPS-initiated latex, but only exerts a negligible effect on the redox-initiated latex [see Figure 5(c)]. The radical generation rate increases with temperature in the KPS-initiated process, and leads to higher radical flux, which results in higher particle numbers in the latex. However, the radicals in the redox-initiated systems are generated by the reduction-oxidation reaction, and the rate is not greatly influenced by the temperature. Figure 5(c) shows a slight decrease in particle number for the redox-initiated latex at higher temperature. This is due to the instability of particles formed in the redox-initiated process. In the redox-initiated process, the higher particle numbers resulted in a larger particle surface area and less surfactant coverage compared to the KPS-initiated process, which indicates that redox-initiated latex are less stable. The higher reaction temperature can decrease the stability of the particles and influence the nucleation process, which can lead to the increase of particle size and the decrease of particle number.

High particle number leads to high reaction rate. In Figure 5(a), a nearly 10 times difference in particle number was observed between the redox-initiated latex (25°C) and the KPS-initiated latex (70°C), but the difference in reaction rate is 4 times (see Figure 2). This difference is partly due to differences in the reaction rate coefficient for the various reaction temperatures. To further confirm that micelle nucleation can produce high particle numbers in the redox-initiated system, the number of micelles above the CMC of SLS were evaluated given a micelle aggregation number[37] of 74 at 25°C and 41 at 70°C. The particle numbers of the redox-initiated latex (N_p=5.54 × 10^{18} with 7.9 m*M* H_2O_2), and the KPS-initiated latex (N_p=3.25 × 10^{17} with 1.7 m*M* KPS) are both less than their micelle number (3.45 × 10^{19} and 6.30 × 10^{19}) with a SLS concentration of 12 m*M* at 25°C and 70°C, respectively, further confirming that the micelle nucleation is operative in the two systems. The radical flux in the redox-initiated system is much higher and form more latex particles from micelles. In addition, homogeneous

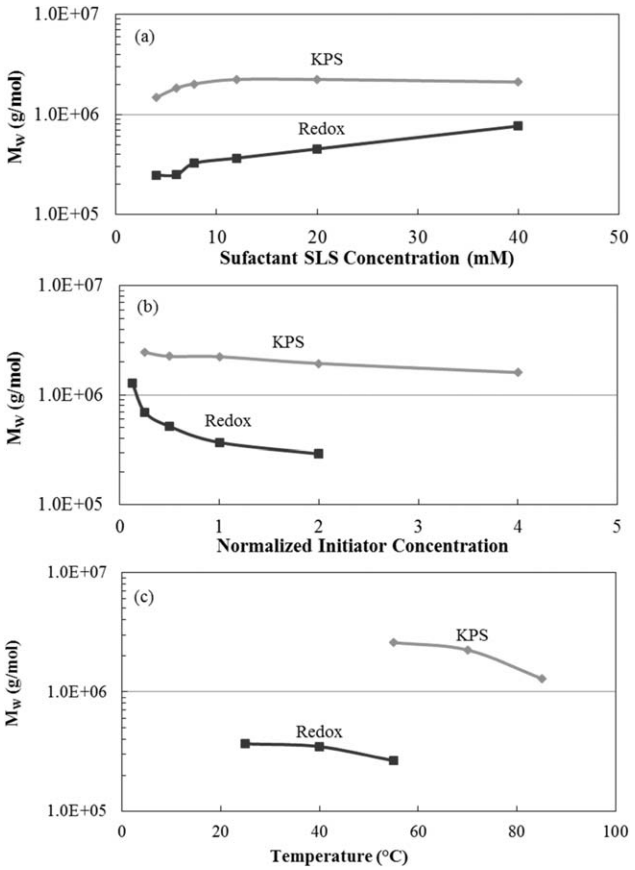

Figure 6. The logarithmic dependence of latex molecular weight, M_W, vs. (a) SLS concentration, (b) normalized initiator strength, and (c) reaction temperatures for KPS and redox-initiated emulsion polymerizations of *n*-BMA. Reactions represented in (a) were the same as in Figure 1, those in (b) were the same as in Figure 2, and those in (c) were the same as in Figure 3. Initiator concentrations were normalized to those values shown in Figure 6(b).

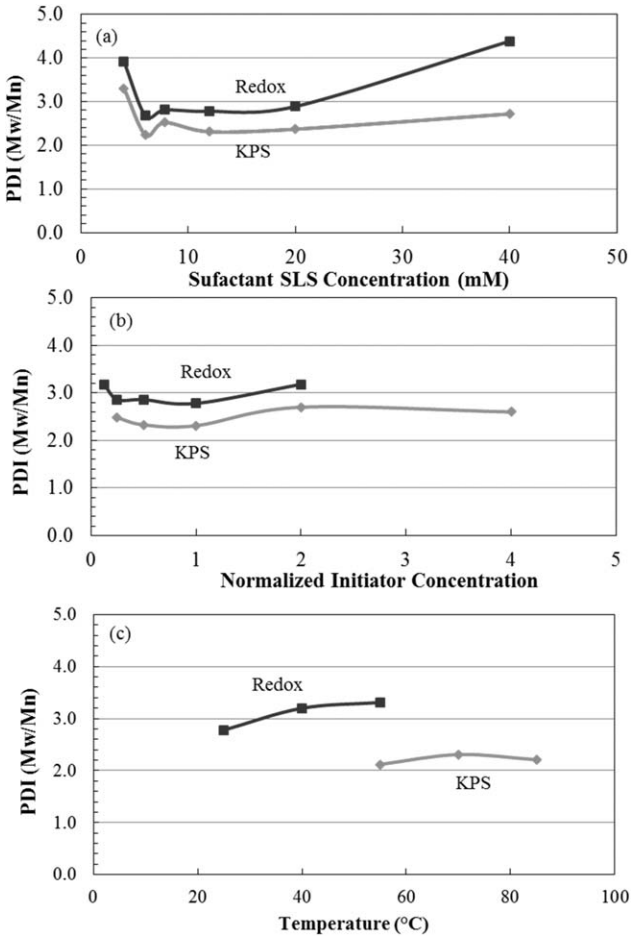

Figure 7. The molecular weight PDI vs. (a) SLS concentration, (b) normalized initiator strength, and (c) reaction temperatures for KPS and redox-initiated emulsion polymerizations of *n*-BMA. Reactions represented in (a) were the same as in Figure 1, those in (b) were the same as in Figure 2, and those in (c) were the same as in Figure 3. Initiator concentrations were normalized to those values shown in Figure 7(b).

nucleation can also play an important role in forming more final latex particles in the redox-initiated reaction due to the presence of a high radical flux and reaction with dissolved monomer in the water phase.

Molecular Weight

Figure 6 illustrates the influence of surfactant concentration, initiator strength and reaction temperature on the molecular weight (weight average) of KPS-initiated latex and redox-initiated latex. The high radical flux in the redox-initiated latex not only results in the formation of latex with much smaller particle size, but also results in the formation of latex with much lower molecular weight. Figure 6(a) shows that the molecular weight increases with surfactant concentration in the redox-initiated latex. The molecular weight of the KPS-initiated latex increases with surfactant concentration, as it is below the CMC, and remains constant with surfactant concentration above the CMC. Higher surfactant concentration leads to greater particle number (as discussed above), and thus results in a lower radical entry rate for each particle indicating higher molecular weight. For the KPS-initiated latex (above the CMC), the radicals per particle may reach equilibrium, and therefore, the molecular weight does not change much. Figure 6(b) shows that the molecular weight decreases with the initiator concentration. Greater initiator concentration generates higher radical flux, and results in a higher radical entry rate for each particle indicating lower molecular weight. Figure 6(c) shows that the molecular weight decreases with the reaction temperatures. The different reaction temperature can influence the radical generation rate, the reaction rate constant, and the particle number. The combination of those three factors influences the molecular weight. Since the molecular weights are significantly different between redox-initiated and KPS-initiated latex, the molecular weights PDI (polydispersity index) were studied. Figure 7 illustrates the molecular weights PDI of KPS-initiated latex and redox-initiated latex. The higher radical flux in redox-initiated system not only generated a lower molecular weight, but also a higher PDI than KPS-initiated latex.

Radical Generation Rate

The radical generation rate plays a very important role in explaining the difference between the KPS-initiated and redox-initiated latex systems. This section provides an analysis of the radical generation mechanism and a quantitative comparison of the radical generation rates of the two initiators. For KPS initiator, the free radicals are generated from thermal decomposition of the initiator, and the generation rate is a function of temperature and initiator concentration.[38] For redox initiator, free radicals are generated from reduction-oxidation reactions. In this work, hydrogen peroxide (H_2O_2) is the oxidant and ascorbic acid (AA) is the reductant. The mechanism of redox initiation is complicated.[39] It can be simplified as oxidant (H_2O_2) reacts with Fe^{2+} to generate radicals and Fe^{3+}. The reducing agent (AA) regenerates Fe^{2+} from Fe^{3+} in order to maintain the generation of radicals. The radical generation rates for two initiators were calculated.[35] Figure 8 presents the dependence of radical generation rates on the initial initiator strengths for redox initiators at 25°C and for KPS at 70°C. The difference in the radical generation rate is more than 10 times, and this is why the redox-initiated latex can have much higher particle number than KPS-initiated latex. In redox-initiated polymerization, the high

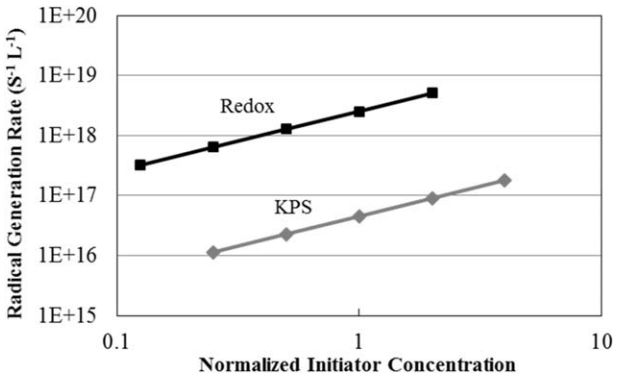

Figure 8. The logarithmic dependence of radical generation rate on the relative initiator strength. The KPS reactions are at 70°C, and the redox reactions are at 25°C. Initiator concentrations were normalized.

radical flux not only results in higher micellar nucleation compared to the KPS-initiated polymerization, but also introduces significant secondary nucleation.[35] Further identification of the nucleation mechanisms in the emulsion polymerization with two initiator systems will be reported in a subsequent paper.

CONCLUSIONS

In this study, redox initiator with a ferrous sulfate catalyst was investigated in the isothermal emulsion polymerization of BMA, and compared to a KPS thermal initiator. In redox-initiated polymerizations, the high radical flux results in the formation of much smaller latex particles and lower molecular weight. The difference in particle number also leads to a significant difference in the reaction rate between the redox-initiated and KPS-initiated systems. The dependence of particle number on surfactant and initiator concentrations reveals that the redox-initiated systems and KPS-initiated systems follow the Smith-Ewart theory and a micellar nucleation mechanism is operative in both reactions. Molecular weight is higher with high surfactant concentration and lower initiator concentration for both systems. Reaction temperature can influence both the particle size and molecular weight.

REFERENCES

1. El-Aasser, M. S.; Sudol, E. D. In Emulsion Polymerization and Emulsion Polymers; Lovell, P. A.; El-Aasser, M. S., Eds.; John Wiley and Son: Chichester, UK, **1997**; Chapter 2, pp 38–41.
2. Chern, C. S. *Prog. Polym. Sci.* **2006**, *31*, 443.
3. The Freedonia Group. World Emulsion Polymers: Industry Study with Forecasts for 2014 & 2019. www.freedoniagroup.com. The Freedonia Group, Cleveland, OH, **2010**, p 4.
4. Hussain, F.; Hojjati, M.; Okamoto, M.; Gorga, R. E. *J Compos. Mater.* **2006**, *40*, 1511.
5. Oh, J. K.; Drumright, R.; Siegwart, D. J.; Matyjaszewski, K. *Prog. Polym. Sci.* **2008**, *33*, 448.
6. Zou, H.; Wu, S.; Shen, *J. Chem. Rev.* **2008**, *108*, 3893.
7. Moinard-Checot, D.; Chevalier, Y.; Briancon, S.; Fessi, H.; Guinebretiere, S. *J. Nanosci. Nanotechnol.* **2006**, *6*, 9.
8. Liu, G.; Qiu, Q.; Shen, W.; An, Z. *Macromolecules* **2011**, *44*, 5237.
9. Monteiro, M. J.; Cunningham, M. F. *Macromolecules* **2012**, *45*, 4939.
10. Smeets, N. M. B.; Moraes, R. P.; Wood, J. A.; McKenna, T. F. L. *Langmuir* **2010**, *27*, 575.
11. Anton, N.; Benoit, J. P.; Saulnier, P. *J. Controlled Release* **2008**, *128*, 185.
12. Solans, C.; Izquierdo, P.; Nolla, J.; Garcia-Celma, M. J. *Curr. Opin. Colloid Interface Sci.* **2005**, *10*, 102.
13. Lawrence, M. J.; Rees, G. D. *Adv. Drug Deliv. Rev.* **2012**, *45*, 89.
14. Kohut-Svelko, N.; Porro, R.; Asua, J. M.; Leiza, J. R. *J. Polym. Sci. Part A: Polym. Chem.* **2009**, *47*, 2917.
15. Goikoetxea, M.; Heijungs, R.; Barandiaran, M. J.; Asua, J. M. *Macromol. React. Eng.* **2008**, *2*, 90.
16. Sarac, A. S. *Prog. Polym. Sci.* **1999**, *24*, 1149.
17. Ming, W.; Jones, F. J.; Fu, S. *Polym. Bull.* **1998**, *40*, 749.
18. Ming, W.; Zhao, Y.; Cui, J.; Fu, S.; Jones, F. N. *Macromolecules* **1999**, *32*, 528.
19. Halnan, L. F.; Napper, D. H.; Gilbert, R. G. *J Chem. Soc.* **1984**, *80*, 2851.
20. Qiu, J.; Gaynor, S. G.; Matyjaszewski, K. *Macromolecules* **1999**, *32*, 2872.
21. Tauer, K.; Muller, H.; Schellenberg, C.; Rosengarten, L. *Colloids Surf. A* **1999**, *153*, 143.
22. Krishnan, S.; Klein, A.; El-Aasser, M. S.; Sudol, E. D. *Macromolecules* **2003**, *36*, 3125.
23. Zhao, F.; Sudol, E. D.; Daniels, E. S.; Klein, A.; El-Aasser, M. S. *J. Appl. Polym. Sci.* **2012**, *126*, 1267.
24. Zhao, F.; Sudol, E. D.; Daniels, E. S.; Klein, A.; El-Aasser, M. S. *J. Appl. Polym. Sci.* **2013**, *130*, 4001.
25. Beuermann, S.; Buback, M.; Davis, T. P.; Gilbert, R. G.; Hutchinson, R. A.; Kajiwara, A.; Klumperman, B. *Macromol. Chem. Phys.* **2000**, *201*, 1355.
26. Geurts, J. M.; Jacobs, P. E.; Muijs, J. G.; Steven Van Es, J. J. G.; German, A. L. *J. Appl. Polym. Sci.* **1996**, *61*, 9.
27. Baxendale, J. H.; Evans, M. C.; Kilham, J. K. *Trans. Faraday Soc.* **1946**, *42*, 668.
28. Barb, W. G.; Baxendale, J. H.; George, P.; Hargrave, K. *Trans. Faraday Soc.* **1951**, *47*, 462.
29. Tsuchida, E.; Hatashita, M.; Makino, C.; Hasegawa, E.; Kimura, N. *Macromolecules* **1992**, *25*, 207.
30. Li, M.; Daniels, E. S.; Dimonie, V.; Sudol, E. D.; El-Aasser, M. S. *Macromolecules* **2005**, *38*, 4183.
31. Smith, W. V.; Ewart, R. H. *J. Chem. Phys.* **1948**, *16*, 592.
32. Song, Z.; Daniels, E. S.; David Sudol, E.; El-Aasser, M. S.; Klein, A. *J. Appl. Polym. Sci.* **2011**, *122*, 203.
33. Collins, E. A. In Emulsion Polymerization and Emulsion Polymers; Lovell, P. A.,El-Aasser, M. S., Eds.; Wiley: Chichester, U. K., **1997**; Chapter 12, p 391.
34. Varela de la Rosa, L. Ph.D. Emulsion Polymerization of Styrene Using an Automated Reaction Calorimeter. Dissertation, Lehigh University, **1996**.
35. Wang, S. Ph.D. Redox-Initiated Adiabatic Emulsion Polymerization. Dissertation, Lehigh University, **2012**.
36. Williams, R. J.; Phillips, J. N.; Mysels, K. J. *Trans. Faraday Soc.* **1955**, *51*, 728.
37. Malliaris, A.; Moigne, J.; Sturm, J.; Zana, R. *J. Phys. Chem.* **1985**, *89*, 2709.
38. Gilbert, R. G. Emulsion Polymerization: A Mechanistic Approach, Academic Press: London, **1995**.
39. Deutsch, J. C. *Anal. Biochem.* **1998**, *255*, 1.